Published in final edited form as:
J Bone Miner Res. 2012 August ; 27(8): 1722–1734. doi:10.1002/jbmr.1619.

Enzyme replacement prevents enamel defects in hypophosphatasia mice

Manisha C. Yadav[1,*], **Rodrigo Cardoso de Oliveira**[1,2,*], **Brian L. Foster**[3,#], **Hanson Fong**[4], **Esther Cory**[5], **Sonoko Narisawa**[1], **Robert L. Sah**[5], **Martha Somerman**[3,#], **Michael P. Whyte**[6], and **José Luis Millán**[1]

Manisha C. Yadav: myadav@sanfordburnham.org; Rodrigo Cardoso de Oliveira: rodrigocardoso@usp.br; Brian L. Foster: blfoster@u.washington.edu; Hanson Fong: hfong@u.washington.edu; Esther Cory: esthercory@ucsd.edu; Sonoko Narisawa: sonokon@sanfordburnham.org; Robert L. Sah: rsah@ucsd.edu; Martha Somerman: martha.somerman@nih.gov; Michael P. Whyte: mwhyte@shrinenet.org; José Luis Millán: millan@sanfordburnham.org

[1]Sanford Children Health Research Center, Sanford-Burnham Medical Research Institute, La Jolla, CA 92037

[2]University of São Paulo, Bauru Dental School, Department of Biological Sciences, Bauru-SP, Brazil

[3]National Institute of Arthritis and Musculoskeletal and Skin Diseases (NIAMS), NIH, Bethesda, MD 20892

[4]Department of Periodontics, University of Washington, Seattle, WA 98195

[5]Department of Bioengineering, University of California, San Diego, La Jolla, CA 92037

[6]Shriners Hospital for Children and Washington University, St. Louis, MO 63131 and 63110, USA

Abstract

Hypophosphatasia (HPP) is the inborn error of metabolism characterized by deficiency of alkaline phosphatase activity leading to rickets or osteomalacia and to dental defects. HPP occurs from loss-of-function mutations within the gene that encodes the tissue-nonspecific isozyme of alkaline phosphatase (TNAP). TNAP knockout (*Alpl*$^{-/-}$, a.k.a. *Akp2*$^{-/-}$) mice closely phenocopy infantile HPP, including the rickets, vitamin B6-responsive seizures, improper dentin mineralization, and lack of acellular cementum. Here, we report that lack of TNAP in *Alpl*$^{-/-}$ mice also causes severe enamel defects, which are preventable by enzyme replacement with mineral-targeted TNAP (ENB-0040). Immunohistochemistry was used to map the spatiotemporal expression of TNAP in the tissues of the developing enamel organ of healthy mouse molars and incisors. We found strong, stage-specific expression of TNAP in ameloblasts. In the *Alpl*$^{-/-}$ mice, histological, μCT, and scanning electron microscopy analysis showed reduced mineralization and disrupted organization of the rods and inter-rod structures in enamel of both the molars and incisors. All of these abnormalities were prevented in mice receiving from birth daily subcutaneous injections of

Corresponding author: José Luis Millán, Ph. D. Sanford Children's Health Research Center, Sanford-Burnham Medical Research Institute, 10901 North Torrey Pines Road, La Jolla, CA 92037; Tel: 858-646-3130; millan@sanfordburnham.org.
*These authors contributed equally to this paper.
#This research was conducted while BLF and MS were at UW.

CONFLICT OF INTEREST
Drs. Whyte and Millán are consultants for Enobia Pharma, now Alexion Pharmaceuticals. All other authors report no conflicts of interest.

Authors' roles: MCY, RCO, and JLM conceived the study. JLM, RS, MS provided funding and designed the experiments. RCO, BLF, HF, EC and SN performed the experiments. JLM, RS, MS and MPW reviewed the data. MCY, MPW and JLM wrote the paper. We wish to thank two anonymous reviewers for their extensive and constructive critiques that guided a considerable improvement of our manuscript.

mineral-targeting, human TNAP (sALP-FcD$_{10}$, a.k.a. ENB-0040) at 8.2 mg/kg/day for up to 44 days. These data reveal an important role for TNAP in enamel mineralization, and demonstrate the efficacy of mineral-targeted TNAP to prevent enamel defects in HPP.

INTRODUCTION

Mineralization of the extracellular matrix (ECM) of skeletal and dental tissues is a complex process, finely regulated by mineral ion availability, phosphatases, and collagenous as well as non-collagenous proteins.[1, 2] Coincident with establishing an extracellular collagenous network in bones and teeth, osteoblasts, chondrocytes, odontoblasts, and cementoblasts all secrete additional non-collagenous proteins that integrate within the collagen fibrillar scaffold and provide additional functionality to the matrix.[3] Along with dental pulp, dentin, and cementum, enamel is one of the four major tissues that make up the tooth organ in vertebrates. Enamel is unique among mineralized tissues because of its especially high mineral content - 96% of which is composed of calcium phosphate in the form of hydroxyapatite [$(Ca_{10}(PO_4)_6(OH)_2$] with water and organic material composing the rest of the tissue. Enamel contains two unique classes of non-collagenous proteins, amelogenins and non-amelogenins.[4] While the role of these proteins is not fully understood, it is believed that they aid in the development of enamel by serving as a framework for minerals to form on.[5] Enamel is produced by ameloblasts in close contact with dentin, until tooth eruption. The synthesis of enamel can be divided into three stages: pre-secretion, secretion, and maturation where the ameloblasts alter their morphology to fulfill the functions of tooth matrix resorption, and mineralization.[6]

Tissue-nonspecific alkaline phosphatase isozyme (TNAP) expression has long been associated with the cells of mineralizing tissues such as cartilage, bone and teeth.[7, 8–10] TNAP plays a crucial role in promoting ECM mineralization by increasing the local availability of phosphate (P_i) needed for hydroxyapatite crystal formation as well as by restricting the concentration of the calcification inhibitor inorganic pyrophosphate (PP_i). Thus, TNAP maintains a P_i/PP_i ratio conducive for mineralization.[11] Deficiency of TNAP activity characterizes hypophosphatasia (HPP), which is an heritable disorder featuring hypomineralization of the skeleton and teeth.[12–14] Clinical manifestations of HPP vary from stillbirth with nearly complete absence of skeletal mineralization to early tooth loss as the only symptom. The typical and striking oral manifestation of HPP is premature loss of primary teeth.[13, 14]

Expression of TNAP by bone, dentin, and cementum has been well characterized by immunohistochemistry and *in situ* hybridization.[15–20] Dysplasia or aplasia of cementum has been well documented histologically in HPP, and this abnormality explains the early exfoliation of deciduous teeth.[21–23] Irregular calcification of dentin and enlarged pulp chambers have also been documented.[17, 23–25] However, while one might suspect that formation of enamel, another highly mineralized tissue, would also depend on the local regulation of P_i/PP_i metabolism, there have been no conclusive reports of enamel defects in HPP patients, although some papers have alluded to enamel hypoplasia in this inborn error of metabolism.[21, 26–28]

In the present study, we mapped the expression of TNAP in the dentition of healthy mice through the maturation stages of ameloblasts and to the stratum intermedium (SI, a 2–3 cell layer adjacent to ameloblasts in the enamel organ) throughout amelogenesis. Furthermore, we found that deficiency of TNAP in *Alpl*$^{-/-}$ mice (*Alpl*, a.k.a. *Akp2* or murine TNAP gene), that recapitulate the infantile form of HPP,[29] leads to enamel defects. Previous studies from our laboratory and from collaborators have shown that enzyme replacement therapy beginning at birth with mineral-targeted human recombinant TNAP (sALP-FcD$_{10}$,

a.k.a. ENB-0040) prevents the skeletal defects and restores the acellular cementum in *Alpl*$^{-/-}$ mice.[30, 31] Here, we show that the benefits of this enzyme replacement extend to the correction of the enamel defect in the *Alpl*$^{-/-}$ mouse model of infantile HPP.

METHODS

Mouse model of infantile HPP

Alpl$^{-/-}$ mice were created by insertion of the Neo cassette into exon 6 of the mouse TNAP gene via homologous recombination, which functionally inactivated the *Alpl* gene resulting in no detectable TNAP mRNA or protein in these mice.[29] *Alpl*$^{-/-}$ mice closely phenocopy human infantile HPP.[29, 32] Similar to these severely affected HPP patients, *Alpl*$^{-/-}$ mice have global deficiency of TNAP activity, together with extracellular accumulation of the TNAP natural substrates PP_i and pyridoxal-5′-phosphate (PLP), and rickets, bowed long bones, and lack of acellular cementum.[29–32] HPP mice have stunted growth and develop vitamin B6-responsive seizures and apnea, and die between 10–12 dpn (day postnatal).[29, 33] Pyridoxine supplementation briefly suppresses their seizures and extends their lifespan, but only until postnatal days 18–22.[33, 34] Therefore, all animals (breeders, nursing mothers and their pups, and weanlings) in this study were given free access to modified laboratory rodent diet 5001 containing increased levels (325 ppm) of pyridoxine. The *Alpl*$^{-/-}$ mice are maintained in a 12.5% C57Bl/6–87.5% 129J background. Homozygous mice are identified at birth (day 0) by analysis of the genome by PCR as published.[35]

Treatment of *Alpl*$^{-/-}$ mice with mineral-targeted TNAP (ENB-0040)

ENB-0040 (sALP-FcD_{10}) is a therapeutic fusion protein composed of soluble recombinant human TNAP (sALP), fused to the constant region of human IgG1 Fc domain (Fc) to facilitate purification, and a C-terminal deca-aspartate motif (D10), that confers targeting to the mineral phase of bone.[30, 31] The expression, purification, and characterization of this fusion protein have been described.[30] Lot number PUR012F01 of ENB-0040 [produced under Current Good Manufacturing Practices (cGMP) formulated at 0.15, 0.6 and 2.5 mg/mL in 25mmol/L sodium phosphate and 150 mmol/L sodium chloride, pH 7.4] was used in the current study. *Alpl*$^{-/-}$ mice were treated with either vehicle or ENB-0040 injections given subcutaneously (SC) daily and divided into 4 groups: Group 1 (Vehicle): treated with vehicle; Group 2 (Tx-0.5): treated with ENB-0040 at 0.5 mg/kg/day; Group 3 (Tx-2.0): treated with ENB-0040 at 2.0 mg/kg/day; and Group 4 (Tx-8.2): treated with ENB-0040 at 8.2 mg/kg/day. Group 5, composed of wild-type (WT) littermate controls, served as reference animals and did not receive injections. The injection regimen and necropsy procedure has been described previously.[35] All treatments began at postnatal day 1, and were repeated daily until the time of necropsy. The necropsy consisted of a gross pathology check, with external pinna collected to confirm the *Alpl*$^{-/-}$genotype. The mandible samples were obtained from archival material form our ENB-0040 dose-response study.[35] Those samples were initially cleaned, fixed in 10% neutral buffered formalin for 3 days at 2 to 8°C, and then transferred to 70% ethanol for storage at 2 to 8°C.[35]

Tissue preparation and histological analyses

The mandibles of treated and untreated mice were demineralized in a solution of 0.05 M ethylenediaminetetraacetic acid (EDTA), pH 7.4 and embedded in paraffin.[36] Sections of 4 μm thickness were cut in a microtome (Microm, model HM 340 E, Germany) and stained with hematoxylin and eosin (H&E) according to conventional techniques. Sagittal sections through the hemi-mandibles provided longitudinally incisor (and surrounding alveolar bone) specimens for comparative histological analyses.

Immunohistochemistry

Immunohistochemistry (IHC) was performed on histological sections of molars and incisors from 15 dpc (day postcoital) to 28 dpn in WT mice. Mouse tissues were harvested as described above and prepared for histology as reported previously.[37] Briefly, mandibles were hemisected sagitally and fixed in Bouin's solution at 4°C overnight. Hemi-mandibles were demineralized (for tissues from 15 dpn) in acetic acid/formalin/sodium chloride (AFS) solution at 4°C. Tissues were paraffin embedded after standard histological processing. Serial sections (5 μm thick) were prepared by rotary microtome and mounted on charged glass slides. TNAP immunohistochemistry was preceded by an unmasking step wherein slides were incubated overnight in 8.0 M guanidine HCl (pH 8.0) solution. A rat monoclonal anti-human TNAP antibody (R&D Systems, Minneapolis, MN) was used with biotinylated secondary antibodies (Vectastain Elite ABC, Vector Labs, Burlingame, CA), and color reactions were developed to a red product using a 3-amino-9-ethylcarbazole (AEC) substrate kit (Vector Labs). Controls for specificity included staining *Alpl* null mouse tissues as well as WT tissues in the absence of primary antibody. For all stages of development, IHC was performed in sections from at least three (n=3) animals, with representative staining chosen for photographs shown in the results section. Digital images were captured with a Nikon Eclipse E400 compound light microscope fitted with a SPOT RT Slider CCD camera (Diagnostic Instruments, Sterling Heights, MI), using Metavue software (Molecular Devices, Sunnyvale, CA).

To detect the presence of ENB-0040 in the treated mice, mandibles were removed from 16 dpn mice ($Alpl^{-/-}$ mice treated with 8.2 mg/kg, WT, and untreated $Alpl^{-/-}$ mice) at necropsy, fixed in 4% PFA/PBS, decalcified in 0.125M EDTA/10% formalin for 5 days, and processed for standard paraffin sectioning. Deparaffinized sections were immersed in 0.37% H_2O_2/methanol for 30 min to inactivate endogenous peroxidase, and treated with 8 M guanidine (pH 10) overnight. After blocking with SuperBlock (Theromo, Rockford, IL), sections were incubated with one mg/ml rat anti- human TNAP antibody (R&D Systems) overnight, followed by a standard ABC staining protocol. Localization of the antibody was detected with DAB (diaminobenzidine) reaction.

Micro-computed Tomography (μCT)

Samples were imaged on a micro-computed tomography scanner, Skyscan 1076 (Kontich, Belgium). Lower mandibles were wrapped in tissue paper that was moistened with Phosphate Buffered Saline (PBS) and scanned at 9 μm voxel size, applying an electrical potential of 50 kVp and current of 200 μA, and using a 0.5 mm aluminum filter. Mineral density was determined by calibration of images against 2 mm diameter hydroxyapatite rods (0.25 and 0.75 gHA/cm^3) with a beam hardening correction algorithm applied during image reconstruction. Analysis was performed on the right side of each jaw. Skyscan software, Dataviewer, CTAn, CTVol (Kontich, Belgium) was used to reorient samples and to obtain maximum intensity projection (MIP) volume data images. Coronal and sagittal sections were taken from the center of the first molar. Additionally, coronal anterior and posterior cross-sections were taken 0.36 mm away from the center coronal section. 3D models were created using a global threshold that included enamel, dentin, and bone structures and a Marching Cubes 33 algorithm for volume visualization. Contours around the mineralized region of the first molar tooth were performed. A global threshold was used to identify either enamel or dentin volumes to calculate the following parameters: total first molar tooth volume (M1V; sum of the enamel and dentin volume), enamel volume (EnV), dentin volume (DeV), percent enamel volume of molar1 (EnV/M1V), percent dentin volume of molar1 (DeV/M1V), enamel mineral density (EnMD) and dentin mineral density (DeMD). Three samples were analyzed per time point and per treatment group; a one-way analysis of variance (ANOVA) was conducted on the resulting microCT parameters (dependent

variables) for each experimental group (treatment and time point as an independent variable). To assess differences between experimental groups for each dependent variable, a Tukey post-hoc test was performed for data that passed the test for homogeneity while the Games-Howell post-hoc test was performed for data with unequal variance. A 0.05 alpha level was used to determine if variations were statistically significant.

Scanning electron microscopy (SEM)

Molars and incisors were mounted in room-temperature-cure epoxy. Similar anatomic regions of the tooth were sought for each sample. Subsequent preparation of epoxy-mounted specimens involved cutting the erupted incisor to expose the mesial surface of the first molar, and the cross-section of the unerupted incisor. The cut surface was then ground further distally to expose the interior of the first molar. Final preparations were polished in 1 μm diamond lapping film followed by etching in 1% phosphoric acid for 30 seconds. All specimens were then mounted on scanning electron microscopy (SEM) stubs, sputter coated with 5 nm of platinum for electron conductivity (SPI Supplies Inc, West Chester, PA), and imaged by an JSM7000F (JEOL-USA, Inc., Peabody, MA) SEM operating at 15 kV in backscattering mode.

RESULTS

TNAP expression in the developing enamel organ

Immunohistochemistry was used to map the spatiotemporal expression of TNAP in the tissues of the developing enamel organ of healthy mouse molars and incisors. In late cap/early bell stage of the molars, prior to differentiation of ameloblasts and odontoblasts, TNAP was not detectable in the teeth, though staining was strong in the surrounding mandibular bone (Fig. 1A). Incisors in the bell stage of tooth development displayed differentiated odontoblasts, which became strongly positive for TNAP during the transition from pre-odontoblasts to odontoblasts (Fig. 1B, C). Pre-ameloblasts were uniformly negative for TNAP, while the overlying SI showed intense TNAP staining. During the late bell stage of both molars and incisors, TNAP expression was localized to odontoblasts as well as the SI and stellate reticulum (SR) of the enamel organ, though secretory stage ameloblasts were TNAP negative (Fig. 1D-F). During tooth eruption and root lengthening, ameloblasts enter the maturation stage, in association with mineralization of the enamel ECM. At 8 dpn, TNAP expression was present in ameloblasts transitioning from the secretory to the maturation stage in the first molars (Fig. 1G and H). By 10 dpn, as all ameloblasts entered the maturation stage, the entire cell layer became positive for TNAP (Fig. 1I). Sagittal sections of the continuously erupting mandibular incisor allowed simultaneous examination of TNAP over the entire course of amelogenesis. Like the molars, TNAP induction in incisor ameloblasts coincided with the transition from the secretory to maturation stage, while the SI was strongly TNAP positive over the entire length of the incisor (Fig. 1J, K). These findings indicate that TNAP is expressed by ameloblasts in a stage-specific manner, as well as being highly expressed by the adjacent SI of the developing enamel organ.

Localization of ENB-0040 to the enamel organ

In order to confirm that, during enzyme replacement therapy, ENB-0040 was localizing to the developing enamel region, we performed immunohistochemistry for human TNAP in incisor sections from mice at age 16 dpn. In $Alpl^{-/-}$ mice treated with 8.2 mg/kg/day ENB-0040, positive staining was observed in the enamel matrix layer during the secretory ameloblast phase (Fig. 2A), unlike untreated $Alpl^{-/-}$ mice, where TNAP immunoreactivity was completely absent (Fig. 2B). Interestingly, this recombinant TNAP localized predominantly to matrix as would be predicted because of the mineral-targeting deca-aspartate motif whereas in WT much stronger TNAP staining was found in the SI and also

odontoblasts (Fig. 2C). In the maturation stage of amelogenesis, TNAP was found in incisor enamel matrix of mice treated with ENB-0040, while WT featured TNAP staining in the SI and ameloblast cell compartments (Supplemental Fig. 1). The specificity of the staining was confirmed using normal rat IgG as negative control (Fig. 2D).

Enamel defects in *Alpl*$^{-/-}$ mice and prevention by a high dose of mineral-targeted TNAP

Further studies were performed on *Alpl*$^{-/-}$ mice treated with vehicle or with mineral-targeted ENB-0040 to determine if TNAP expression is important for the process of enamel formation and mineralization. Hematoxylin and eosin (H & E) staining showed an absence of enamel formation on incisors of *Alpl*$^{-/-}$ mice at 23 dpn (Supplemental Fig. 2A, B and C). Treatment with the lower doses of ENB-0040 (0.5 mg/kg/day, Tx-0.5 group and 2.0 mg/kg/day, Tx-2.0 group) did not lead to visible improvement in amelogenesis at this age. Visual observation of the histological sections showed that dentin thickness was compromised in untreated *Alpl*$^{-/-}$ mice and in the Tx-0.5 group, whereas the Tx-2.0 group showed increased dentin thickness (Supplemental Fig. 2A, B, C).

The Tx-2.0 group exhibited improvement in enamel formation by day 44, and the highest tested dose of ENB-0040 (8.2 mg/kg/day, Tx-8.2 group) completely rescued the enamel defect phenotype by this age (Fig. 3B and C). The thickness of enamel and dentin layers of the Tx-8.2 group appeared similar to those in the WT group. The layer of ameloblasts showed abnormal morphology in the Tx-2.0 group compared to the WT group in the pre-secretory, secretory, and maturation phases, and the adjacent SI was also noticeably disrupted in this group. Ameloblasts appeared detached from the ECM layer and, along with other cells of the enamel organ, accumulated to form a disorganized multilayered structure, in contrast to the well-defined layers of polarized ameloblasts and SI cells in the WT controls (Fig. 3A and B, arrows). However, in the Tx-8.2 group, ameloblasts appeared elongated and polarized, formed an enamel ECM indistinguishable from WT animals, and were bounded by an organized SI cell layer, as in the WT (Fig. 3A and B, arrow).

μCT images of the mandible at early age (20–23 dpn) (Supplemental Fig. 3) revealed a striking reduction of enamel mineralization in the first and second molars and the incisor crown analog in *Alpl*$^{-/-}$ mice. Confirming the histological observations, the 0.5 mg/kg/day dose had minimal impact on improving enamel formation, while the 2.0 mg/kg/day dose resulted in a recognizable enamel layer in molars and incisors by μCT. Mineralization defects in alveolar bone also showed slight improvement in the Tx-2.0 group; the alveolar ridge, which appeared devoid of mineralization in *Alpl*$^{-/-}$ mice, was perceptibly more mineralized in the Tx-2.0 group. Sagittal and full jaw views (Supplemental Fig. 3D and F) showed an improvement in mineralization at the incisal socket with the higher dose tested at 23 dpn (Tx-2.0). At 23 dpn, molar roots and incisor root analogs, however, still suffered from little to no mineralization, and were indistinguishable from adjacent soft tissues such as pulp and periodontal ligament.

Quantitatively, at the early time point (20–23 dpn), absolute and relative enamel volumes varied between experimental groups, while the total volume of enamel and dentin (M1V) as well as mineral densities (EnMD and DeMD) were similar between groups (supplemental Table 1 and 2). While EnV, EnV/M1V and EnMD were not significantly different between vehicle and treatment groups (Tx-0.5 or Tx-2.0), the higher treatment dose (Tx-2.0 vs Tx-0.5) led to higher EnV ($p<0.034$) and EnV/M1V ($p<0.001$). At this early age, both treatment doses (Tx-0.5 and Tx-2.0) differed from WT in effects on EnV ($p<0.001$ and $p<0.037$, respectively) and EnV/M1V (both, $p<0.001$). Although DeV/M1V varied between experimental groups (inverse to EnV/M1V), the dentin parameter, DeV, at this time point did not vary significantly between groups.

At 44 dpn (Fig. 4), mineralized enamel was present on molars in the Tx-2.0 and Tx-8.2 groups as shown by μCT. Interestingly, incisor enamel mineralization for both treatment groups appeared to lag behind the WT group, in that coronal sections (Fig. 4A–C) showed less mineralized enamel in incisors versus WT, and sagittal sections (Fig. 4D) indicated that enamel mineralization occurred more incisally compared to WT. Surrounding bone appeared more mineralized as the treatment dose increased from 2.0 to 8.2 mg/kg/day (Fig. 4A–F). In addition, molar roots and incisor root analogs, which are severely affected in *Alpl*$^{-/-}$ mice, were markedly improved in both treatment groups at this age. In fact, after the longest treatment period and highest dose of ENB-0040 (Tx-8.2 group at 44 dpn), tooth mineralization appeared similar to that of the WT samples.

At this late time point (44 dpn), the Tx-2.0, Tx-8.2, and WT groups showed no significant differences in any parameters, M1V as well as absolute and relative enamel and dentin parameters (Enamel parameters – Tx-2.0 vs WT: $p = 0.35$ for EnV, $p = 0.18$ for EnV/M1V, $p = 0.99$ for EnMD; Tx-8.2 vs WT: $p = 1.0$ for EnV, $p = 0.87$ for EnV/M1V $p = 1.0$ for EnMD; Dentin parameters – Tx-2.0 vs WT: $p = 0.52$ for DeV, $p = 0.18$ for DeV/M1V, $p = 1.00$ for DeMD; Tx-8.2 vs WT: $p = 0.95$ for DeV, $p = 0.87$ for DeV/M1V $p = 0.99$ for DeMD) (supplemental Table 1 and 2).

Comparison (Supplemental Table 2) between early (23 dpn) and late (44 dpn) time points was possible only for the WT and Tx-2.0 treatment groups, and we found that the increased age and treatment duration (44 dpn vs 23 dpn) led to substantially higher DeV (each, $p<0.001$) and M1V ($p<0.001$ and $p<0.003$, respectively). However, the increase in DeV/M1V with age and treatment duration was substantially more for WT than Tx-2.0. The age-associated differences suggest a developmental delay that could be partially corrected over time (Fig. 4D, E, F and Supplemental Fig. 3).

SEM showed the expected, well-decussated (intersected) enamel rods and inter-rod structure in both molars and incisors of WT mice (Fig. 5). Enamel organization reflects the creation of ribbons (rods) of self-assembled enamel proteins secreted by ameloblasts. Rods are normally seen largely surrounded by distinct inter-rods, and the apical surface of each rod blends into an inter-rod to form a continuum, producing a ‘fish scale’ appearance. However, the *Alpl*$^{-/-}$ mice showed a marked disturbance in this enamel architecture, including disruption of the rod boundaries, rod decussation, and disruption of the crystallite on the rods. Overall, SEM indicated that TNAP deletion in the mouse resulted in defects in enamel structural organization at 20 dpn, namely a highly disorganized enamel rod and inter-rod structure. These molar and incisor enamel organizational abnormalities in *Alpl*$^{-/-}$ mice were slightly improved in those animals treated with the lowest dose of ENB-0040 (Tx-0.5 group), with considerably greater improvement seen in the Tx-2.0 group at 34 dpn. (Fig. 6A, B). Both treatment groups featured recognizable enamel rods, with better organization of rods and inter-rod structure, especially in the Tx-2.0 group. SEM indicated markedly improved enamel rod and inter-rod architecture in both incisors and molars in the Tx-8.2 group, with enamel in the incisors of the Tx-8.2 group, in particular, appearing similar to WT at 44 dpn (Fig. 7). Decussated rod structures could be seen in the Tx-2.0 and Tx-8.2 groups, though both groups also featured patches of clearer rod organization and less well defined rod decussation. Thus, SEM analysis indicated that *Alpl*$^{-/-}$ mice had defects of both enamel mineralization and architecture, and that enzyme replacement treatment with 8.2 mg/kg/day ENB-0040 (Tx-8.2 group) largely prevented these defects and rescued the enamel phenotype by 44 dpn.

DISCUSSION

Hypophosphatasia (HPP) is the rare and sometimes fatal metabolic bone disease characterized by defective mineralization of the skeleton and dentition, and caused by loss-of-function mutation(s) within the gene that encodes TNAP.[14] The biochemical hallmark is subnormal ALP activity in serum. However, the expressivity of HPP ranges remarkably and features a clinical picture that spans a rapidly fatal perinatal form with profound skeletal hypomineralization and respiratory compromise at birth, to complications from osteomalacia or poorly understood dental manifestations presenting late in adult life. The severe perinatal and infantile forms of HPP are inherited as autosomal recessive traits, whereas the milder forms of this inborn-error-of-metabolism are transmitted as autosomal dominant or recessive traits.[14] More than 250 deactivating mutations (~ 80% missense defects) at the *ALPL* (*TNAP, TNSALP*) locus have been identified in HPP patients world wide (http://www.sesep.uvsq.fr/03_hypo_mutations.php).

Understandably, HPP features a considerable range of signs, symptoms, and complications from the underlying dento-osseous disease. These depend on the overall severity, which is largely reflected by the age at HPP presentation. Perinatal HPP is the most pernicious form, and can manifest *in utero* with profound skeletal hypomineralization that results at birth in caput membranaceum, deformed or shortened limbs, and acute respiratory failure. Long-term survival is rare. Infantile HPP presents as a seemingly acquired disorder before 6 months of life.[38] Postnatal development of these patients can appear normal until the onset of poor feeding and inadequate weight gain, and clinical manifestations of rickets. Vitamin B_6-responsive epilepsy can occur, which is a harbinger of a lethal outcome. In childhood HPP, premature loss of deciduous teeth (i.e., before age five years) is often the earliest sign of the disorder.[21–23, 39] In nearly all HPP patients, incisors are shed first; occasionally, almost the entire primary dentition is exfoliated prematurely. Dental radiographs sometimes show the enlarged pulp chambers and root canals characteristic of the “shell teeth” of rickets.[24, 25, 39, 40] HPP patients may also experience delayed walking, have a characteristic waddling gait, complain of stiffness and pain, and have appendicular muscle weakness consistent with a non-progressive myopathy. In the adult form, HPP typically presents during middle age. Frequently, however, there is a remote history of rickets, premature loss of deciduous teeth, or early loss of adult dentition. Odonto-HPP, the mildest form, is diagnosed when dental disease is the only clinical abnormality, and radiographic and/or histological studies reveal no evidence of skeletal disease. Loss of the deciduous teeth in HPP has been attributed to a deficiency of cementum[24, 41–43] with impaired dentin formation.[21, 24] However, no report has referred to enamel defects in HPP patients or in TNAP knockout mice.

In the present study, we defined the normal pattern of TNAP expression during enamel formation in healthy WT mice. We mapped TNAP expression to the maturation stages of ameloblasts and to the stratum intermedium (SI) throughout amelogenesis. The SI is a 2–3 cell-thick supra-ameloblast layer that arises from the odontogenic epithelium. While the function(s) of the SI remain(s) unknown, this layer has been implicated in cell signaling events,[45] and is in prime location to invest and support ameloblasts during amelogenesis. The SI has been noted to express TNAP, and there has been speculation on the function of this enzyme in ameloblast differentiation or mineral ion transport.[17, 46] Ameloblasts, during the secretory stage, produce and secrete enamel matrix proteins responsible for directing enamel appositional growth and initial mineralization of enamel rods.[6] High TNAP expression is present during the transition of ameloblasts to the maturation stage when ameloblasts direct the removal of matrix proteins and facilitate the transport of mineral ions to increase the width and thickness of preexisting hydroxyapatite crystals, suggesting a role for TNAP in the maturation of enamel. A previously reported[18, 44] pattern of biphasic

TNAP expression in both pre-secretory/secretory ameloblasts as well as maturation stage ameloblasts, was not observed in our study. TNAP expression was not seen in ameloblasts during initial enamel mineralization, when the appositional width of enamel is completed, although the adjacent odontoblasts and SI cells were strongly TNAP positive, in accordance with previous reports.[18, 44] Throughout crown formation, the SI featured remarkably consistent and intense TNAP expression. The lack of significant TNAP expression in ameloblasts during initial enamel mineralization while the adjacent SI strongly expresses the enzyme suggests a role for the SI in creating conditions for propagation of enamel mineralization. Expression of TNAP by the SI and by maturation-stage ameloblasts may be essential for enamel matrix mineralization. Deficiency of TNAP in HPP would result in disruption of this process, contributing to enamel mineral defects such as enamel hypoplasia.

We have shown here that ENB-0040 reaches the enamel organ during the secretory and maturation phases, in the treated *Alpl*$^{-/-}$ mice. SEM of *Alpl*$^{-/-}$ mice demonstrates a lack of organization of rod and inter-rod structure of enamel. μCT data shows that at 23 dpn, ENB-0040 has dose-dependent normalizing effects on both absolute and relative enamel volumes. Histological analysis of *Alpl*$^{-/-}$ mice shows reduced enamel mineralization both in molars and incisors, loss of polarization of ameloblasts that are important for enamel matrix formation, and even complete lack of enamel formation in the absence of TNAP. The fact that patients with odonto-HPP typically have the most mild reductions of serum TNAP levels, suggests that tooth formation is the most sensitive developmental process requiring TNAP function.[13, 30, 31] Previous studies of cementum have demonstrated the sensitivity of this tissue to changes in the local P_i/PP_i ratio,[47] and the ability of mineral-targeted TNAP to preserve acellular cementum in *Alpl*$^{-/-}$ mice has further validated that premise.[31] Here too, the ability of ENB-0040 to preserve the structural integrity of enamel supports the notion that the enamel organ is also under direct regulation by the extracellular P_i/PP_i ratio and that TNAP plays a crucial role in this regulation.

Previously, transgenic mice wherein enamel mineralization was disturbed have featured disorganization and dysmorphism of the ameloblast cell layer. This includes disruptions of enamel specific factors like amelogenin and matrix metalloproteinase 20,[48, 49] as well as disruptions in other factors likely related to ameloblast differentiation.[50, 51] Based on our current observations and these previous reports, we speculate that loss of TNAP affects the orderly process of ameloblast differentiation by one of two ways: First, loss of TNAP may impair enamel matrix mineralization, which may secondarily affect ameloblast organization in relation to forming enamel matrix surface. Second, TNAP may be required for proper transition of ameloblasts to the maturation stage, based on the pattern observed by immunohistochemistry. These outcomes need not be mutually exclusive, as TNAP may play a role both in matrix mineralization and functional cell differentiation, as it does in other mineralizing cells, e.g. osteoblasts.[52, 53] In fact, the complete role for TNAP in mineralizing cells may not be understood at present, and our studies focused on ameloblasts, which produce mineralized enamel by a mechanism quite distinct from the fibrillar collagen-based mineralized tissues bone, dentin, and cementum, may provide further insight on the necessity for TNAP in all hard tissues. The ability of recombinant mineral-targeted TNAP to rescue ameloblast morphology and enamel mineralization is likely by correction of the cell-matrix interface and/or ameloblast differentiation. The substantial expression of TNAP in the SI and the potential role of this tissue in enamel organ and ameloblast function is an additional area of interest under investigation.

Ameloblasts undergo several differentiation processes: the pre-secretory, secretory, and maturation stages.[54] In the pre-secretory stage, the basement membrane matrix separates the dental epithelium and mesenchymal pre-odontoblasts.[55, 56] At the secretory stage, the basement membrane matrix disappears, and enamel matrix replaces the basement membrane

to support and regulate the secretory ameloblast cells.[57] The secretory stage ameloblasts produce and secrete specific proteins in the enamel matrix that are later replaced by calcium and phosphorus (hydroxyapatite crystals) during the maturation stage for enamel formation. The principal components of the enamel matrix synthesized are amelogenins and ameloblastins.[57] Amelogenin-null mice[58] exhibit a phenotype similar to human X-linked amelogenesis imperfecta in which ameloblast differentiation is normal, but an abnormally thin enamel layer is formed. It has been suggested that amelogenins are essential for the organization of the crystal pattern and regulation of thickness of enamel. Ameloblastin, also known as amelin and sheathlin, is a tooth-specific glycoprotein, which represents the most abundant enamel matrix protein.[59–61] Unlike amelogenin, ameloblastin localizes near the cell surface and not in the deep enamel matrix layer.[62] Recently, it was reported that transgenic mice over-expressing ameloblastin in ameloblasts resemble amelogenesis imperfecta, confirming the importance of ameloblastin in enamel formation.[63] Enamel defects in the $Alpl^{-/-}$ mice could in part be due to low production or inactivation of either amelogenins or ameloblastins. Indeed, ameloblastin null mice[64] show similar phenotypic abnormalities to those documented here for the $Alpl^{-/-}$ mice. In ameloblastin null mice, ameloblasts are detached from the matrix and subsequently lose cell polarity, resume proliferation, and form multicell layers. Thus, ameloblastin is a cell adhesion molecule essential for amelogenesis, and maintains the differentiation state of secretory-stage ameloblasts by binding to ameloblasts and inhibiting proliferation. The function and structure of ameloblastin remain unclear, and there are no known proteins with similar primary sequences. It has been shown that human ameloblastin exists as two splice variants,[65, 66] and that mutations at a phosphorylation site lead to ameloblastoma (epithelial odontogenic tumor).[65] These reports suggest that the different splice variants of ameloblastin might have different phosphorylation status, and thus function differently. It could be hypothesized that TNAP modulates the phosphorylation status of ameloblastin in ameloblasts, and in the absence of TNAP, ameloblastins become inactive and lead to deformed enamel matrix production. Such a function of TNAP in enamel formation would be analogous to a role of TNAP in modulating the phosphorylation state of osteopontin during bone mineralization (Narisawa et al., In Preparation).

An important conclusion from our study is that enzyme replacement therapy with mineral-targeted TNAP (ENB-0040), when administered daily at a dose of 8.2 mg/kg/day, prevents the enamel defects observed in untreated $Alpl^{-/-}$ mice. Previously, we showed that ENB-0040 prevents the skeletal defects as well as the cementum and dentin abnormalities of $Alpl^{-/-}$ mice.[30, 31, 35] Our current data extend the potential benefits from this therapeutic principle to also include restoration of enamel structure and function in this animal model and perhaps in HPP patients.

In summary, TNAP is highly expressed in ameloblasts during the maturation stages and in the surrounding tissue throughout enamel development. $Alpl^{-/-}$ mice show severe enamel defects both in the molars and incisors. Hence, in addition to abnormalities in cementum and dentin formation, enamel defects can be added to the disease complications suffered by HPP patients. Our study provides further evidence for the robustness of enzyme replacement therapy with ENB-0040 that can prevent the skeletal abnormalities and cementum defects in this mouse model of HPP, but also reach the enamel organ, a notoriously avascular tissue. In fact, ENB-0040 treatment appears to be beneficial for the dento-osseous disease of severely affected infants and children with HPP.[67]

Supplementary Material

Refer to Web version on PubMed Central for supplementary material.

Acknowledgments

This work was funded by grants DE12889, AR47908 and AR53102 from the National Institutes of Health, USA. Rodrigo C. de Oliveira was a recipient of a fellowship from CAPES (4176-09-0).

References

1. Giachelli CM. Inducers and inhibitors of biomineralization: lessons from pathological calcification. Orthod Craniofac Res. 2005; 8:229–231. [PubMed: 16238602]
2. Murshed M, Harmey D, Millán JL, McKee MD, Karsenty G. Unique coexpression in osteoblasts of broadly expressed genes accounts for the spatial restriction of ECM mineralization to bone. Genes Dev. 2005; 19:1093–1104. [PubMed: 15833911]
3. McKee, MD.; Sodek, J. In The Osteoporosis Primer. Henderson, JE.; Goltzman, D., editors. Cambridge University Press; Cambridge, UK: 2000. p. 46-63.
4. Termine JD, Belcourt AB, Christner PJ, Conn KM, Nylen MU. Properties of dissociatively extracted fetal tooth matrix proteins. I. Principal molecular species in developing bovine enamel. J Biol Chem. 1980; 255:9760–9768. [PubMed: 7430099]
5. Ten, Cate AR. Oral Histology: development, structure, and function. 7. Mosby, an affiliate of Elsevier Inc; 2008.
6. Simmer JP, Papagerakis P, Smith CE, Fisher DC, Rountrey AN, Zheng L, Hu JC. Regulation of dental enamel shape and hardness. J Dent Res. 2010; 89:1024–1038. [PubMed: 20675598]
7. Robison R, Macleod M, Rosenheim AH. The possible significance of hexose phosphoric esters in ossifications. IX. Calcification in vitro. Biochem. 1930; 24:1927–1941.
8. Bonting SJ, Nuki K. Comparative studies of the developing hamster tooth by quantilative ultramicrochemical fechnique and by histochemical staining methods. Ann Histochim. 1963; 8:79–88. [PubMed: 14173108]
9. Woltgens JH, Bonting Sl, Bijvoet OLM. Relationship of inorganic pyrophosphatase and alkaline posphatase activities in hamster molars. Calcif Tissue Res. 1970; 5:333–343. [PubMed: 5469613]
10. Larmas M, Thesleff I. Biochemical study of changes in non-specific alkaline phosphomonoesterase activity during mouse tooth ontogeny. Arch Oral Biol. 1980; 25:791–797. [PubMed: 6944000]
11. Meyer JL. Can biological calcification occur in the presence of pyrophosphate? Arch Biochem Biophys. 1984; 231:1–8. [PubMed: 6326671]
12. Fraser D. Hypophosphatasia. Am J Med. 1957; 22:730–746. [PubMed: 13410963]
13. Whyte, MP. Hypophosphatasia: nature's window on alkaline phosphatase function in humans. In: Bilezikian, JP.; Raisz, LG.; Martin, TJ., editors. Principles of bone biology. 3. Academic Press; San Diego, California: 2008. p. 1573-1598.
14. Whyte, MP. Hypophosphatasia. In: Glorieux, FH.; Jueppner, H.; Pettifor, J., editors. Pediatric Bone. 3. Elsevier (Academic Press); San Diego, California: 2012. p. 771-794.
15. Hasselgren G, Franzén A, Hammarström LE. Histochemical characterization of alkaline phosphatase in developing rat teeth and bone. Scand J Dent Res. 1978; 86:325–336. [PubMed: 281754]
16. Groeneveld M, Everts V, Beertsen W. Alkaline phosphatase activity in the periodontal ligament and gingiva of the rat molar: its relation to cementum formation. J Dent Res. 1995; 74:1374–1381. [PubMed: 7560388]
17. Wöltgens JH, Lyaruu DM, Bronckers AL, Bervoets TJ, Van Duin M. Biomineralization during early stages of the developing tooth in vitro with special reference to secretory stage of amelogenesis. Int J Dev Biol. 1995; 39:203–212. [PubMed: 7626408]
18. Hoshi K, Amizuka N, Oda K, Ikehara Y, Ozawa H. Immunolocalization of tissue-non-specific alkaline phosphatase in mice. Histochem Cell Biol. 1997; 107:183–191. [PubMed: 9105889]
19. Beertsen W, VandenBos T, Everts V. Root development in mice lacking functional tissue-nonspecific alkaline phosphatase gene: inhibition of acellular cementum formation. J Dent Res. 1999; 78:1221–1229. [PubMed: 10371245]

20. van den Bos T, Beertsen W. Alkaline phosphatase activity in human periodontal ligament: age effect and relation to cementum growth rate. J Periodontal Res. 1999; 34:1–6. [PubMed: 10086880]
21. Hu J, Plaetke R, Mornet E, Zhang C, Sun X, Thomas H, Simmer J. Characterization of a family with dominant hypophosphatasia. Eur J Oral Sci. 2000; 108:189–194. [PubMed: 10872988]
22. Bruckner RJ, Rickles NH, Porter DR. Hypophosphatasia with premature shedding of teeth and aplasia of cementum. Oral Surg Oral Med Oral Pathol. 1962; 15:1351–1369. [PubMed: 14016153]
23. El-Labban NG, Lee KW, Rule D. Permanent teeth in hypophosphatasia: light and electron microscopic study. J Oral Pathol Med. 1991; 20:352–360. [PubMed: 1895252]
24. Beumer J 3rd, Trowbridge HO, Silverman S Jr, Eisenberg E. Childhood hypophosphatasia and the premature loss of teeth. A clinical and laboratory study of seven cases. Oral Surg Oral Med Oral Pathol. 1993; 35:631–640. [PubMed: 4512507]
25. Jedrychowski JR, Duperon D. Childhood hypophosphatasia with oral manifestations. J Oral Med. 1979; 34:18–22. [PubMed: 289724]
26. Macfarlane J, Swart J. Dental aspects of hypophosphatasia: a case report, family study, and literature review. Oral Surg Oral Med Oral Pathol. 1989; 67:521–526. [PubMed: 2654797]
27. Watanabe H, Umeda M, Seki T, Ishikawa I. Clinical and laboratory studies of severe periodontal disease in an adolescent associated with hypophosphatasia. A case report. J Periodontol. 1993; 64:174–180. [PubMed: 8385214]
28. Reibel A, Manière M, Clauss F, Droz D, Alembik Y, Mornet E, Bloch-Zupan A. Orodental phenotype and genotype findings in all subtypes of hypophosphatasia. Orphanet J Rare Dis. 2009; 4:6. [PubMed: 19232125]
29. Narisawa S, Fröhlander N, Millán JL. Inactivation of two mouse alkaline phosphatase genes and establishment of a model of infantile hypophosphatasia. Dev Dyn. 1997; 208:432–446. [PubMed: 9056646]
30. Millán JL, Narisawa S, Lemire I, Loisel TP, Boileau G, Leonard P, Gramatikova S, Terkeltaub R, Pleshko Camacho N, McKee MD, Crine P, Whyte MP. Enzyme replacement therapy for murine hypophosphatasia. J Bone Miner Res. 2008; 23:777–87. [PubMed: 18086009]
31. McKee MD, Nakano Y, Masica DL, Gray JJ, Lemire I, Heft R, Whyte MP, Crine P, Millán JL. Enzyme replacement prevents dental defects in a mouse model of hypophosphatasia. J Dent Res. 2011; 90:470–476. [PubMed: 21212313]
32. Fedde KN, Blair L, Silverstein J, Coburn SP, Ryan LM, Weinstein RS, Waymire K, Narisawa S, Millán JL, MacGregor GR, Whyte MP. Alkaline phosphatase knockout mice recapitulate the metabolic and skeletal defects of infantile hypophosphatasia. J Bone Miner Res. 1999; 14:2015–2026. [PubMed: 10620060]
33. Waymire KG, Mahuren JD, Jaje JM, Guilarte TR, Coburn SP, MacGregor GR. Mice lacking tissue non-specific alkaline phosphatase die from seizures due to defective metabolism of vitamin B-6. Nat Genet. 1995; 11:45–51. [PubMed: 7550313]
34. Narisawa S, Wennberg C, Millán JL. Abnormal vitamin B6 metabolism in alkaline phosphatase knockout mice causes multiple abnormalities, but not the impaired bone mineralization. J Pathol. 2001; 193:125–133. [PubMed: 11169525]
35. Yadav MC, Lemire I, Leonard P, Boileu G, Blond L, Beliveau M, Cory E, Sah RL, Whyte MP, Crine P, Millán JL. Dose response of bone-targeted enzyme replacement of murine hypophosphatasia. Bone. 2011; 49:250–256. [PubMed: 21458605]
36. Oliveira RC, Oliveira FH, Cestari TM, Taga R, Granjeiro JM. Morphometric evaluation of the repair of critical-size defects using demineralized bovine bone and autogenous bone grafts in rat calvaria. Clinical Oral Implants Res. 2008; 19:749–754. [PubMed: 18720554]
37. Foster BL, Nagatomo KJ, Bamashmous SO, Tompkins KA, Fong H, Dunn D, Chu EY, Guenther C, Kingsley DM, Rutherford RB, Somerman MJ. The Progressive Ankylosis Protein Regulates Cementum Apposition and Extracellular Matrix Composition. Cells Tissues Organs. 2011; 194:382–405. [PubMed: 21389671]
38. Whyte, MP. Hypophosphatasia. In: Scriver, CR.; Beaudet, AL.; Sly, WS.; Valle, D., editors. The metabolic and molecular bases of inherited disease. 8. McGraw-Hill; New-York NY, USA: 2001. p. 5313-5329.

39. Olsson A, Matsson L, Blomquist HK, Larsson A, Sjodin B. Hypophosphatasia affecting the permanent dentition. J Oral Pathol Med. 1996; 25:343–347. [PubMed: 8887081]
40. Liu H, Li J, Lei H, Zhu T, Gan Y, Ge L. Genetic etiology and dental pulp cell deficiency of hypophosphatasia. J Dent Res. 2010; 89:1373–1377. [PubMed: 20924064]
41. Kjellman M, Oldfelt V, Nordenram A, Olow-Nordenram M. Five cases of hypophosphatasia with dental findings. Int J Oral Surg. 1973; 2:152–158. [PubMed: 4203655]
42. Lundgren T, Westphal O, Bolme P, Modéer T, Norn J. Retrospective study of children with hypophosphatasia with reference to dental changes. Scand J Dent Res. 1991; 99:357–364. [PubMed: 1754836]
43. van den Bos T, Handoko G, Niehof A, Ryan LM, Coburn SP, Whyte MP. Cementum and dentin in hypophosphatasia. J Dent Res. 2005; 84:1021–1025. [PubMed: 16246934]
44. Hotton D, Mauro N, Lézot F, Forest N, Berdal A. Differential expression and activity of tissue-nonspecific alkaline phosphatase (TNAP) in rat odontogenic cells in vivo. J Histochem Cytochem. 1999; 47:1541–1552. [PubMed: 10567438]
45. Koyama E, Wu C, Shimo T, Iwamoto M, Ohmori T, Kurisu K, Ookura T, Bashir MM, Abrams WR, Tucker T, Pacifici M. Development of stratum intermedium and its role as a Sonic hedgehog-signaling structure during odontogenesis. Dev Dyn. 2001; 222:178–191. [PubMed: 11668596]
46. Lézot F, Descroix V, Hotton D, Mauro N, Kato S, Berdal A. Vitamin D and tissue non-specific alkaline phosphatase in dental cells. Eur J Oral Sci. 2006; 114(Suppl 1):178–182. [PubMed: 16674682]
47. Nociti FH Jr, Berry JE, Foster BL, Gurley KA, Kingsley DM, Takata T. Cementum: a phosphate-sensitive tissue. J Dent Res. 2002; 81:817–821. [PubMed: 12454094]
48. Bartlett JD, Skobe Z, Lee DH, Wright JT, Li Y, Kulkarni AB. A developmental comparison of matrix metalloproteinase-20 and amelogenin null mouse enamel. Eur J Oral Sci. 2006; 114(Suppl 1):18–23. discussion 39–41, 379. [PubMed: 16674657]
49. Wazen RM, Moffatt P, Zalzal SF, Yamada Y, Nanci A. A mouse model expressing a truncated form of ameloblastin exhibits dental and junctional epithelium defects. Matrix Biol. 2009; 28:292–303. [PubMed: 19375505]
50. Osawa M, Kenmotsu S, Masuyama T, Taniguchi K, Uchida T, Saito C. Rat wct mutation prevents differentiation of maturation-stage ameloblasts resulting in hypo-mineralization in incisor teeth. Histochem Cell Biol. 2007; 128:183–193. [PubMed: 17636316]
51. Toth K, Shao Q, Lorentz R, Laird DW. Decreased levels of Cx43 gap junctions result in ameloblast dysregulation and enamel hypoplasia in Gja1Jrt/+ mice. J Cell Physiol. 2010; 223:601–609. [PubMed: 20127707]
52. Millán, JL. Mammalian Alkaline Phosphatases: From Biology to Applications in Medicine and Biotechnology. Weinheim, Germany: Wiley-VCH; 2006.
53. Foster BL, Nociti FH, Swanson EC, Matsa-Dunn D, Berry JE, Cupp CJ. Regulation of cementoblast gene expression by inorganic phosphate in vitro. Calcif Tissue Int. 2006; 78:103–112. [PubMed: 16467974]
54. Fincham AG, Moradian-Oldak J, Simmer JP. The structural biology of the developing dental enamel matrix. J Struct Biol. 1999; 126:270–299. [PubMed: 10441532]
55. Thesleff I, Barrach HJ, Foidart JM, Vaheri A, Pratt RM, Martin GR. Changes in the distribution of type IV collagen, laminin, proteoglycan, and fibronectin during mouse tooth development. Dev Biol. 1981; 81:182–192. [PubMed: 7461285]
56. Adams JC, Watt FM. Regulation of development and differentiation by the extracellular matrix. Development. 1993; 117:1183–1198. [PubMed: 8404525]
57. Smith CE. Cellular and chemical events during enamel maturation. Crit Rev Oral Biol Med. 1998; 9:128–161. [PubMed: 9603233]
58. Gibson CW, Yuan ZA, Hall B, Longenecker G, Chen E, Thyagarajan T, Sreenath T, Wright JT, Decker S, Piddington R. Amelogenin-deficient mice display an amelogenesis imperfecta phenotype. J Biol Chem. 2001; 276:31871–31875. [PubMed: 11406633]
59. Cerny R, Slaby I, Hammarström L, Wurtz T. A novel gene expressed in rat ameloblasts codes for proteins with cell binding domains. J Bone Miner Res. 1996; 11:883–891. [PubMed: 8797107]

60. Fong CD, Slaby I, Hammarström L. Amelin: an enamel-related protein, transcribed in the cells of epithelial root sheath. J Bone Miner Res. 1996; 11:892–898. [PubMed: 8797108]

61. Krebsbach PH, Lee SK, Matsuki Y, Kozak CA, Yamada KM, Yamada Y. Full-length sequence, localization, and chromosomal mapping of ameloblastin. A novel tooth-specific gene. J Biol Chem. 1996; 271:4431–4435. [PubMed: 8626794]

62. Nanci A, Zalzal S, Lavoie P, Kunikata M, Chen W, Krebsbach PH, Yamada Y, Hammarstrom L, Simmer JP, Fincham AG. Comparative immunochemical analyses of the developmental expression and distribution of ameloblastin and amelogenin in rat incisors. J Histochem Cytochem. 1998; 46:911–934. [PubMed: 9671442]

63. Paine ML, Wang HJ, Luo W, Krebsbach PH, Snead ML. A transgenic animal model resembling amelogenesis imperfecta related to ameloblastin overexpression. J Biol Chem. 2003; 278:19447–19452. [PubMed: 12657627]

64. Fukumoto S, Kiba T, Hall B, Iehara N, Nakamura T, Longenecker G. Ameloblastin is a cell adhesion molecule required for maintaining the differentiation state of ameloblasts. J Cell Biol. 2004; 167:973–983. [PubMed: 15583034]

65. Perdigao PF, Gomez RS, Pimenta FJGS, De Marco L. Ameloblastin gene (AMBN) mutations associated with epithelial odontogenic tumors. Oral Oncol. 2004; 40:841–846. [PubMed: 15288841]

66. Toyosawa S, Fujiwara T, Ooshima T, Shintani S, Sato A, Ogawa Y, Sobue S, Ijuhin N. Cloning and characterization of the human ameloblastin gene. Gene. 2000; 256:1–11. [PubMed: 11054529]

67. Whyte MP, Greenberg CR, Salman NJ, Bober MB, McAlister WH, Wenkert D, Van Sickle BJ, Simmons JH, Edgar TS, Bauer ML, Hamdan MA, Bishop N, Lutz RE, McGinn M, Craig S, Moore JN, Taylor JW, Cleveland RH, Cranley WR, Lim R, Thacher TD, Mayhew JE, Downs M, Millán JL, Skrinar AM, Crine P, Landy H. Enzyme Replacement Therapy In Life-Threatening Hypophosphatasia. N Eng J Med. 2012; 366:904–913.

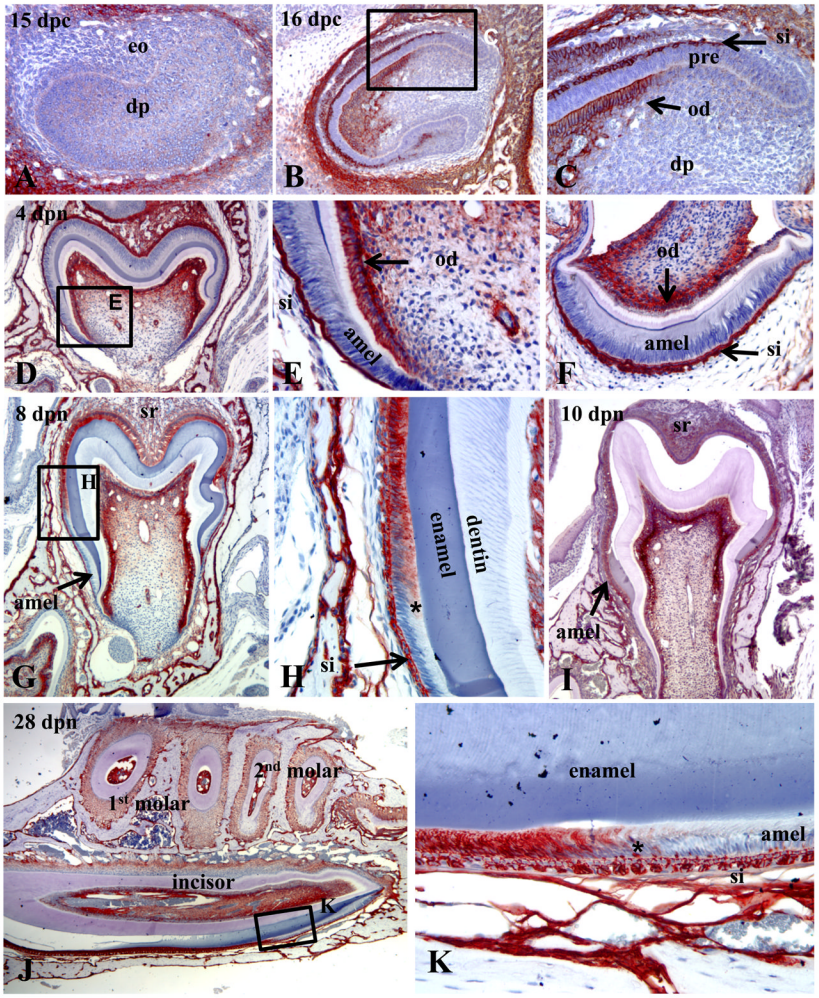

Figure 1.

Immunohistochemistry showing the spatiotemporal expression of TNAP in the healthy (WT) developing enamel organ of fetal and postnatal mice. (A) No TNAP expression is observed in the late cap/early bell stage of the E15 mandibular first molar, before the appearance of the enamel and dentin matrices. (B, C) At E16, the developing maxillary incisor shows TNAP expression in odontoblasts as well as the stratum intermedium (SI) of the enamel organ. Pre-ameloblasts were not observed to be positive for TNAP. (D, E) Localization of TNAP to odontoblasts, as well as SI and stellate reticulum at the 4 dpn mandibular first molar bell stage. (F) Coronal sections of the mandibular incisor at 4 dpn confirms TNAP expression in the SI, but not in ameloblasts during the bell stage. (G, H) By 8 dpn, induction of TNAP expression was localized to ameloblasts of the first mandibular molar, in association with transition (*) from secretory-stage to maturation-stage. ameloblasts (I) By 10 dpn, when the entire ameloblast layer of the first mandibular molar had transitioned to maturation stage, the entire layer was found to be TNAP positive. (J, K) Sagittal sections of the mandibular incisor at 26 dpn confirmed induction of TNAP in ameloblasts at transition (*) from the secretory to maturation stage, while the SI is TNAP-positive over the entire course of incisor amelogenesis and eruption. eo = enamel organ; dp = dental papilla; pre = pre-ameloblasts; SI = stratum intermedium; od = odontoblasts; amel = ameloblasts; SR = stellate reticulum.

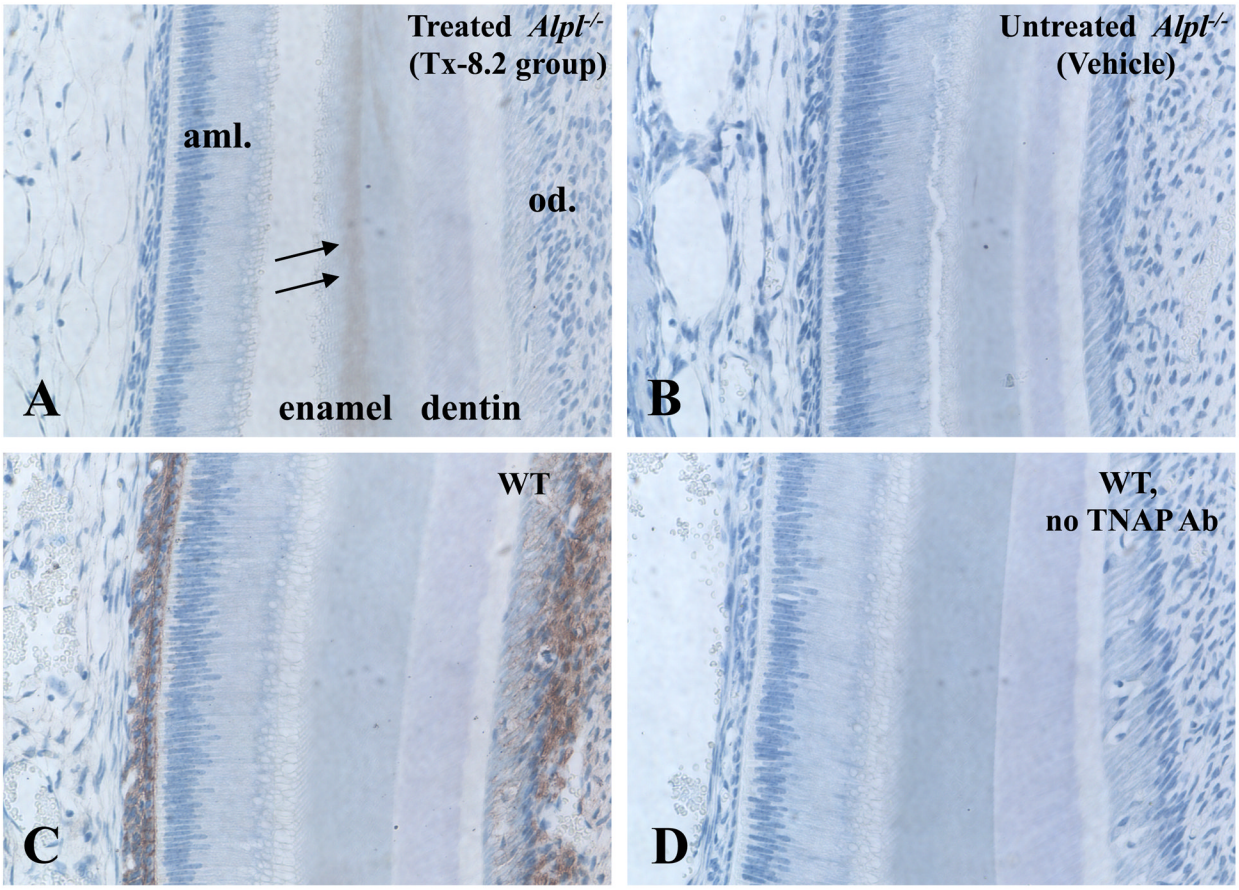

Figure 2.

ENB-0040 localization to the developing enamel region. Immunohistochemistry of TNAP was performed in incisor sections from mice at age 16 dpn. During the secretory ameloblast phase (A) TNAP was found to be present in incisor enamel matrix of mice treated with ENB-0040, while (B) TNAP was absent from untreated *Alpl*$^{-/-}$ mice. (C) WT mice featured TNAP staining in SI and odontoblasts. (D) Specificity of results was confirmed using normal rat IgG as a control for the non-specific staining.

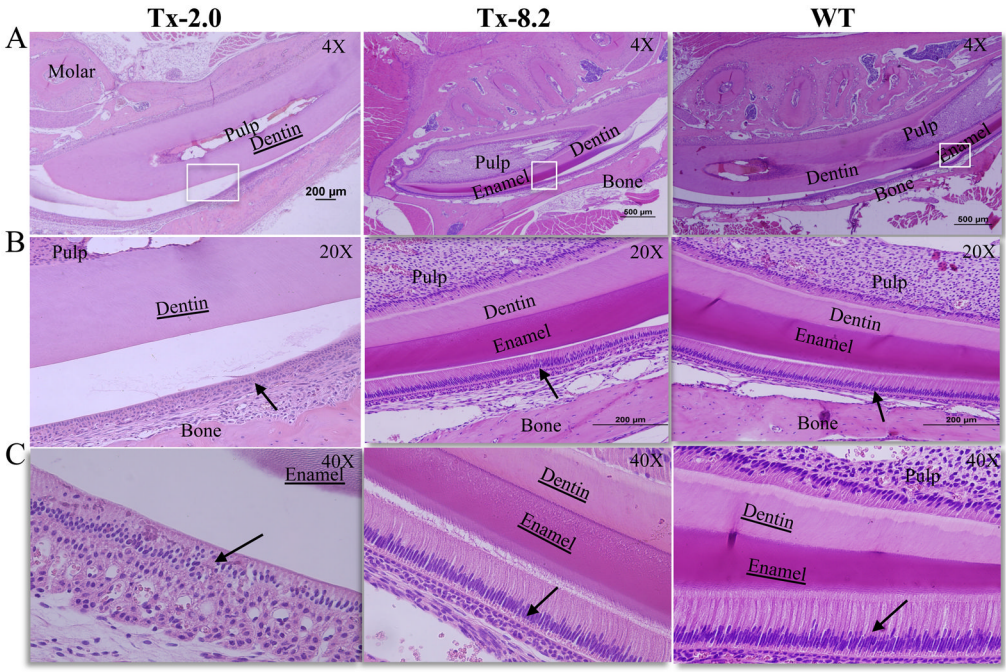

Figure 3.

Histological analysis of enamel development in molars and incisors of *Alpl*$^{-/-}$ mice with enzyme replacement treatment. H&E staining of mandibles from (A, B and C) 44 dpn *Alpl*$^{-/-}$mice given Tx 2.0, Tx-8.2 and untreated WT mice. Enamel seemed to be already formed in the Tx-2.0 group, and the TX-8.2 group shows complete prevention of enamel defects at 44 days of age. At this stage the mature enamel of the incisor in Tx-8.2 group was comparable to that in WT mice. Loss of organization of ameloblasts and disorganized enamel matrix ECM production in the Tx-2.0 group was drastically improved in the Tx-8.2 group, as the enamel organ was rescued to resemble what is seen in WT mice (B and C, arrows). White boxes indicate the corresponding region from A to B and C.

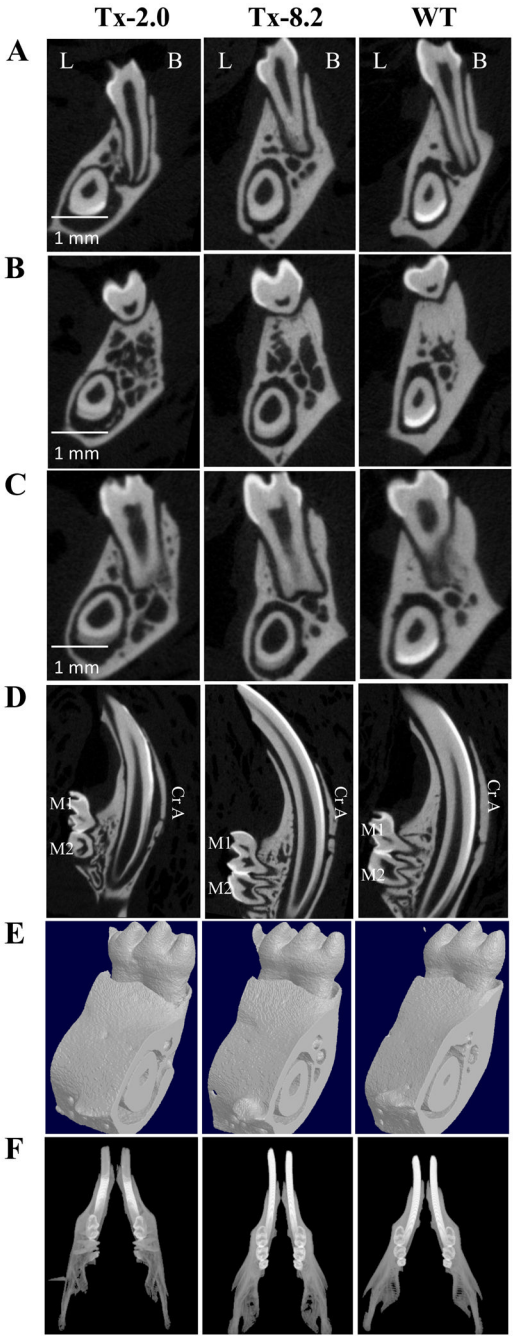

Figure 4.

μCT analysis of *Alpl*$^{-/-}$ teeth at 44 days of age in the Tx-2.0, Tx-8.2 groups and WT mice. (A) Coronal view, 1st mandibular molar (mesial root); (B) Coronal view, 1st mandibular molar (furcation area); (C) Coronal view, 1st mandibular molar (distal root); (D) Sagittal view, mandibular molars and incisor; (E) 3D volumes and (E) full jaw view. Note that the Tx-8.2 group shows complete correction of mineralization in both the molars and incisors, which look similar to that in the WT mice. (L: lingual, B: Buccal, Cr A: Crown analogue in incisor)

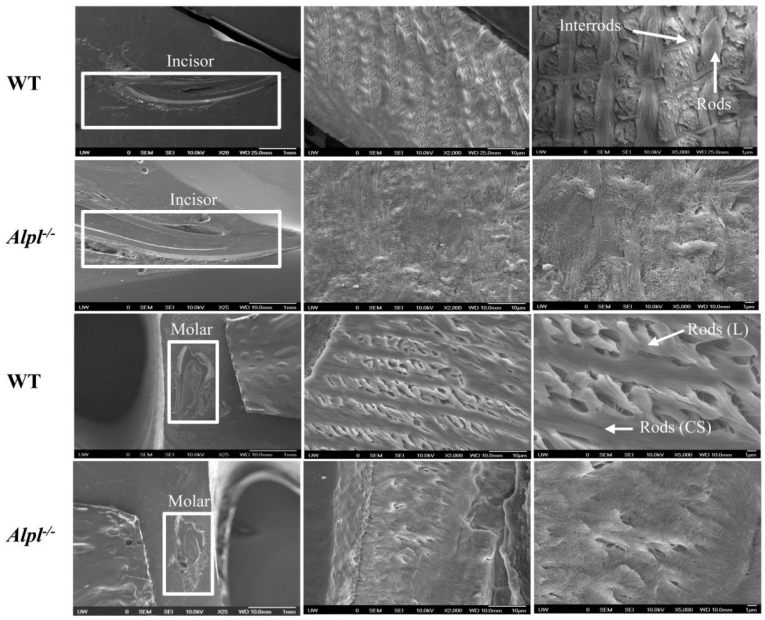

Figure 5.

Scanning electron microscopy (SEM) analysis of incisors (top) and molars (bottom) of WT and *Alpl*$^{-/-}$ mice at 20 dpn. The SEM images showed well-decussated enamel rods and inter-rod in the molar crowns and crown analogs of incisors of WT mice. Note that there is lack of rod-interrod organization in the *Alpl*$^{-/-}$ mice. The images were taken in the erupted part of the tooth.

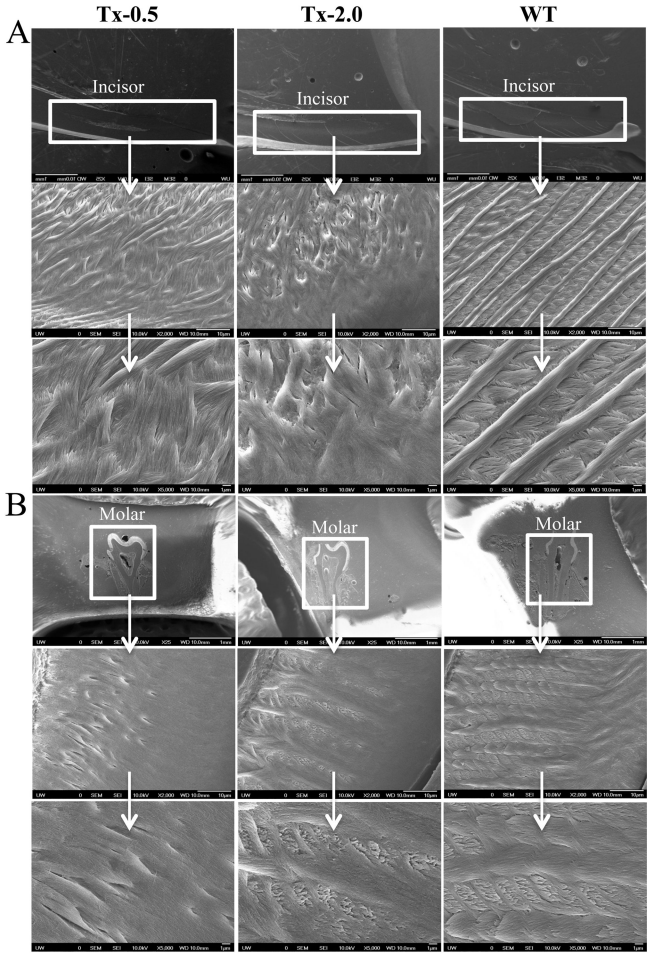

Figure 6.

SEM analysis showing enamel in (A) erupted incisors and (B) molars of 34 dpn *Alpl*$^{-/-}$ mice in the Tx-0.5, Tx-2.0, and untreated WT mice. These images show the preservation of the rods and inter-rod organization in enamel of both incisors and molars with treatment. The appearance of decussated rods is seen already in the Tx-2.0 group, similar to WT mice.

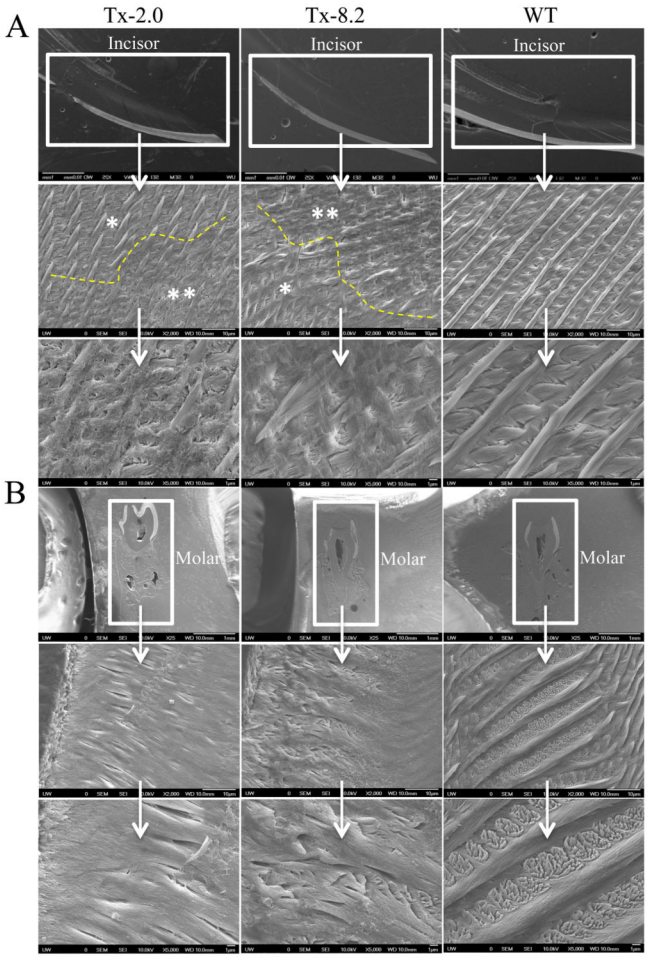

Figure 7.

SEM analysis showing enamel in (A) erupted incisor and (B) molars of 44 dpn *Alpl*$^{-/-}$mice in the Tx-2.0, Tx-8.2, and untreated WT mice. These images show improvement in rod structure in the enamel of both incisors and molars already in the Tx-2.0 group, although there are still patches of clearer rod organization (*) and less well-defined rod decussation (**). The Tx-8.2 group shows much greater improvement in the molars at 44 dpn.